Hypoxia imaging-directed radiation treatment planning

J.G. Rajendran[1, 2, 4], K.R.G. Hendrickson[2], A.M. Spence[3], M. Muzi[1], K.A. Krohn[1, 2], D.A. Mankoff[1]

[1] Department of Radiology, University of Washington Seattle, WA, USA
[2] Department of Radiation Oncology, University of Washington Seattle, WA, USA
[3] Department of Neurology, University of Washington Seattle, WA, USA
[4] Division of Nuclear Medicine, University of Washington Box 356113 Seattle, WA 98195, USA

Published online: 9 June 2006

Abstract. Increasing evidence supports the role of the tumor microenvironment in modulating cancer behavior. Tissue hypoxia, an important and common condition affecting the tumor microenvironment, is well established as a resistance factor in radiotherapy. Increasing evidence points to the ability of hypoxia to induce the expression of gene products, which confer aggressive tumor behavior and promote broad resistance to therapy. These factors suggest that determining the presence or absence of tumor hypoxia is important in planning cancer therapy. Recent advances in PET hypoxia imaging, conformal radiotherapy, and imaging-directed radiotherapy treatment planning now make it possible to perform hypoxia-directed radiotherapy. We review the biological aspects of tumor hypoxia and PET imaging approaches for measuring tumor hypoxia, along with methods for conformal radiotherapy and image-guided treatment, all of which provide the underpinnings for hypoxia-directed therapy. As a case example, we review emerging data on PET imaging of hypoxia to direct radiotherapy.

Keywords: Tissue hypoxia – Radiotherapy – PET – Image-guided treatment

Eur J Nucl Med Mol Imaging (2006) 33:S44–S53
DOI 10.1007/s00259-006-0135-1

Introduction: the biology of tumor hypoxia and hypoxia imaging

Hypoxia as a feature of the tumor microenvironment

As tumors grow, a number of microenvironmental changes evolve that are largely dictated by abnormal vasculature and metabolism. This is primarily caused by unregulated cellular growth, resulting in a greater demand on nutrients for energy metabolism. One of the most important of such microenvironmental changes is hypoxia, reduced oxygenation in tissues. Levels of oxygen range across a continuum from normal levels (euoxia or normoxia) to total lack of oxygen (anoxia). The tissue oxygen levels, commonly reported as Po_2, can reach as low as 5 mmHg and cells can still survive and adapt to the environment. Since Thomlinson and Gray described the mechanistic basis of hypoxia development as a function of distance from a capillary [1], much research has gone in to circumventing the cure-limiting influence of hypoxia. With technical advances in hypoxia imaging and radiation therapy, the time is ripe for actively revisiting the hypoxia problem and to overcome its cure-limiting effects.

Biological consequences of hypoxia

In spite of high microvessel density, aggressive tumors can have high levels of hypoxia [2]. Irrespective of the level of perfusion or status of the vasculature in a tumor, hypoxia induces changes that reflect homeostatic attempts to maintain adequate oxygenation by increasing extraction from blood and by inducing cells to adapt by developing more aggressive survival traits through expression of new proteins. A number of hypoxia-related genes are responsible for these changes and are mediated via downstream transcription factors that have been identified [3–5] and are relevant to treatment and imaging [6]. The primary cellular oxygen sensing mechanism appears to be mediated by a heme protein that uses O_2 as a substrate to catalyze hydroxylation of proline in a segment of the α-subunit of hypoxia-inducible factor 1 (HIF1α). This leads to rapid degradation of HIF1α under normoxic conditions [7]. In the absence of O_2, HIF1α accumulates and forms a heterodimer with HIF1β that is transported to the nucleus and promotes "hypoxia-responsive" genes, resulting in a cascade of genetic and metabolic events in an effort to mitigate the effects of hypoxia on cellular energetics [8, 9]. Increased glucose transporter (GLUT) activity and increased expression of glycolytic enzymes are responsible

J.G. Rajendran (✉)
Division of Nuclear Medicine,
University of Washington,
Box 356113 Seattle, WA 98195, USA
e-mail: rajan@u.washington.edu
Tel.: +1-206-5984248

for much of the increased glucose uptake associated with hypoxia, which can be as high as twofold [10, 11]. Although glycolysis is increased by hypoxia, hypoxia and glucose metabolism will not follow a simple relationship, a fact that needs to be considered in the clinical and imaging characterization of tumor biology and its treatment and that compromises the utility of ^{18}F-fluorodeoxyglucose (FDG) positron emission tomography (PET) as a surrogate for hypoxia [12].

Hypoxia and cancer therapy

Radiobiologists have long taught that low levels of intracellular oxygen result in poor response to radiation therapy. Oxygen is important for "fixing," in the sense of making permanent the radiation-induced cytotoxic products in tissues. In its absence, the free radicals formed by ionizing radiation recombine without producing the anticipated cellular damage [13–15]. As a result, radiation oncologists have been confronted by the fact that hypoxic tumors are not effectively eradicated with conventional doses of radiation. Clinical and preclinical experience indicates that it can take three times as much photon radiation dose to cause the same cytotoxic effect in hypoxic cells as compared to normoxic cells [15–17]. However, cancer treatment schemes introduced to circumvent the cure-limiting consequences of hypoxia have led to disappointing results [18], mainly associated with problems of lack of widespread availability or serious clinical toxicity, or have simply been ineffective in human trials. While focal hypoxia in a tumor can be treated with boost radiation using conformal methods [19, 20], a more diffuse hypoxia will benefit from hypoxic cell toxins/sensitizers, which are hypoxia-activated pro-drugs that can exhibit synergistic toxicity when used with radiation and chemotherapy [21, 22]. Lack of non-invasive and simple hypoxia assays has delayed ready application of hypoxia-directed radiotherapy. Nuclear imaging with hypoxia-specific tracers should play an important role in selecting patients who might benefit from this treatment [23].

PET radiopharmaceuticals for hypoxia imaging

To be maximally successful, hypoxia-directed imaging and treatment should target both chronic hypoxia and hypoxia resulting from transient interruption of blood flow [24]. The assay should reflect intracellular P_{O_2} rather than blood flow or some consequence of O_2 on subsequent biochemistry. The observed temporal heterogeneity in tissue P_{O_2} suggests that a secondary effect, such as intracellular redox status, will not be as relevant to cancer treatment outcome as the intracellular partial pressure of O_2. Other desirable characteristics for an ideal clinical hypoxia assay include: (a) simple and non-invasive method, (b) non-toxic, (c) rapid and easy to perform with consistency between laboratories and (d) the ability to quantify without the need for substantial calibration of the detection instrumentation. PET hypoxia imaging satisfies all these criteria. Even though both single-photon emission computed tomography (SPECT) and PET radiopharmaceuticals have been developed for hypoxia imaging, PET technology provides the advantage of better image quality and the ability to quantify different aspects of hypoxia.

Misonidazole, a lipophilic 2-nitroimidazole derivative initially used as a hypoxic cell sensitizer, binds covalently to intracellular molecules at levels that are inversely proportional to intracellular oxygen concentration below about 20 mmHg. It is a derivative whose uptake in hypoxic cells is dependent on the sequential reduction of the nitro group on the imidazole ring [25]. This mechanism requires that the cell be alive and undergoing electron transport in order to provide the electron that initiates the bioreduction. The one-electron reduction product is an unstable radical anion that will either give up its extra electron to O_2 or pick up a second electron. In the absence of an alternative electron acceptor such as oxygen, the nitroimidazole continues to accumulate electrons to form the hydroxylamine alkylating agent and become trapped within the alive but O_2-deficient cell. ^{18}F-fluoromisonidazole (FMISO) is a PET imaging version [26] that is a highly stable and robust radiopharmaceutical [27]. After extensive clinical validation, it remains the most commonly used agent for hypoxia PET imaging [5, 28–32].

A number of alternative 2-nitroimidazole derivatives have been evaluated that affect the partition coefficient and plasma clearance rate. These have ranged from a fluoroethyl version and ones with multiple F-atom substitutions to carbohydrate derivatives [33]. ^{18}F-FAZA is probably the most widely studied of this group [34]. It is likely that these 2-nitroimidazoles will yield images similar to ^{18}F-FMISO, although the farther the partition coefficient is from unity, the more likely blood flow will be a secondary factor in its biodistribution kinetics, both uptake and washout.

Another hypoxia imaging PET tracer, Cu-ATSM, shows retention in hypoxic areas [35–37], but through an entirely different mechanism. This radiopharmaceutical has rapid washout from normoxic areas. It is a useful imaging agent for identifying regions of tissue that have higher levels of reducing agents such as NADH as a consequence of hypoxia. This mechanism is distinct from that for the nitroimidazoles, in that the copper agent reflects a consequence of hypoxia rather than the actual P_{O_2}. A recent study evaluated the difference between ^{18}F-FMISO and ^{64}Cu-ATSM in an animal model using micro-PET [38].

In evaluating different hypoxia tracers, it is important to keep in mind that the intent is not tumor detection but rather hypoxia measurement. Therefore, the utility of a radiopharmaceutical should be judged not on the basis of image quality but on its ability to quantify regional tissue hypoxia without other complicating factors such as blood flow. This implies that another imaging modality, such as computed tomography (CT) as part of PET/CT or FDG PET will be used to identify the tumor sites that should be queried for the presence of hypoxia, rather than using the hypoxia agent to both localize the tumor and determine whether it is hypoxic.

Image-guided radiotherapy directed at hypoxia

General concepts for image-guided radiotherapy

Imaging has always played a major role in radiation treatment planning for delineating the target volume (tumor) and critical normal tissues. The aim of radiation treatment planning is to deliver the highest possible radiation to the tumor with minimal radiation to critical normal tissues in order to maintain the maximum therapeutic ratio. The physical location and extent of the tumor are localized as the gross tumor volume (GTV) with sufficient margins to account for the biological extension of the tumor type, largely based on clinical experience to account for the biological behavior of cancer. This clinical target volume (CTV) is used to generate the planning target volume (PTV), which accounts for other uncertainties caused by patient movement and radiation delivery. Historically, two-dimensional imaging such as radiography and ultrasound played important roles for this purpose. With the advent of CT scanners, a quick transition was made and dedicated CT simulators are now housed in most radiation oncology departments.

Advances in radiation treatment planning and delivery

The explosive growth in computer-assisted three-dimensional planning within the last decade has allowed radiation oncologists to perform complicated treatment planning and three-dimensional conformal radiation therapy (3DCRT) and intensity-modulated radiation therapy (IMRT). Potential clinical improvements include less toxicity and the promise of safely delivering higher doses of radiation with sharper margins. Dose escalation has improved local control and survival [39, 40]. In principle, concomitant boost can be delivered using a small 'field-within-a-field' technique if hypoxia is identified on pretherapy scans. Advances in IMRT permit dynamic shaping of the radiation beam during treatment. Treatments using inverse planning systems have the potential advantage of a more conformal dose distribution and have the ability to deliver a much higher tumor dose while limiting the normal tissue toxicity [41].

The technical aspects of delivery of radiation therapy have also undergone a revolution over the past two decades. Three-dimensional treatment planning software allows the physician to design radiation treatment beams that conform to the shape of the tumor and reduce dose to normal tissues [42]. Likewise, advances in computerized beam delivery systems with 360° gantry rotations, patient couch rotations, and multileaf collimators permit placement of treatment beams from several directions, converging near the center of the tumor, with irregular beam edges well defined by the multileaf collimators. Advances in patient immobilization are allowing more reproducible setup and alignment of the patient, reducing positional uncertainty to a few millimeters.

Planning techniques such as 3DCRT and IMRT utilize beams directed at the target from multiple angles with field openings shaped to match the beam's-eye view of the target. IMRT adds a layer of refinement that can achieve even greater conformity of dose than 3DCRT. In IMRT, each beam is subdivided into beamlets, typically 1×1 cm^2 or smaller in size, evenly distributed over the cross-section of the beam. Each beamlet can have a different intensity, and thereby create a complex, three-dimensional dose distribution within the patient. The clinician describes the treatment goals in terms of dose objectives or constraints to various parts of the body: targets to receive high doses and organs at risk to receive low doses. A cost function is defined by how close the computed doses are to the prescription doses for the volumes. Optimization engines and search routines iteratively alter the intensity of each beamlet to minimize the total cost function. In this way, an optimal set of beamlets is found and can be recreated for the patient using a multileaf collimator system on the treatment machine [43–47].

IMRT can produce sharp dose gradients between targets and normal tissues and can even generate concave dose distributions to avoid nearby or adjacent critical structures, such as the spinal cord or optic nerves in head and neck cases. This type of dose distribution is not possible with standard planning or 3DCRT. This makes selective boost of specific subvolumes such as hypoxic regions possible without causing significant normal tissue damage. However, the sharp dose gradients that characterize IMRT plans require that the targets be precisely and accurately defined to avoid missing the tumor and compromising successful radiation treatment [48, 49].

More accurate delineation of the target is needed. Currently treatment volumes are based on the tumor-induced change in the contrast CT or magnetic resonance (MR) images and on a subjective clinical judgement as to the extension of microscopic disease. MR provides improved information regarding normal soft tissue structures. PET and MR spectroscopy hold out promise for localizing regions that are biologically distinct, e.g., hypoxic regions or regions with relatively high amounts of DNA replication. Coregistration and fusion of these images with the CT dataset used for radiation therapy planning provides unique and complementary information. Further, this additional biological information overlaid on the anatomic images of the patient leads to the possibility of defining subvolumes of the tumor that might be appropriate for treatment to a higher dose [50]. IMRT-based planning can be used to safely escalate the dose to these subvolumes without added morbidity [51].

PET to guide radiotherapy

With rapid advances in molecular imaging and the availability of modern integrated units such as PET/CT, it is now possible to use functional information to introduce another dimension to radiation treatment planning beyond the physical information. This is the biological target volume (BTV)

[52]. 3D treatment plans make it possible to perform conformal treatment plans with abilities to deliver non-uniform boost doses to smaller volumes within the GTV based on biological imaging. A number of novel tracers are available for PET imaging and include ^{18}F-FDG, ^{18}F-fluorothymidine (FLT) and ^{18}F-FMISO to evaluate metabolism, proliferation and hypoxia, respectively [53–55]. These molecular imaging methods provide us with the ability to characterize tumor and its microenvironment and plan individualized treatments. The most important of these microenvironmental factors is tumor hypoxia, as discussed above. Hypoxic cells require more radiation dose for the same cytotoxic effect as normoxic cells [13] and hypoxic cells acquire aggressive traits that contribute to poorer prognosis [54, 56]. Thus, an additional boost dose of radiation to hypoxic subvolumes might improve tumor control and benefit the patient. The difficulties associated with earlier hypoxia evaluation methods, such as oxygen electrodes, are largely overcome by molecular imaging methods to identify, localize, and quantify hypoxia in tumors non-invasively. The advances in imaging and radiation treatment planning provide a unique opportunity to deliver a hypoxia-directed radiation boost.

Stand-alone PET scanners have played a pivotal role in characterizing hypoxia. However, the problems associated with image fusion limited their utility in radiation treatment planning. Modern PET/CT scanners have the potential for projecting functional target volume onto the treatment planning CT scan and are obviating the image fusion difficulties seen with dedicated PET scanners. Concepts for using the biological imaging information in designing a radiation treatment plan are rapidly evolving [57–59], and benefits from fused PET and CT images are maximized when obtained in the same position in one sitting. These co-registered images are then used to develop complex treatment plans using IMRT [60].

Accurate target volume delineation is critical to successfully incorporate the information from molecular imaging into radiation treatment planning. One approach uses quantitative information, e.g., threshold images or parametric maps, that can increase the accuracy and has the potential to eliminate the subjective aspects from this process [61, 62]. In order to use PET/CT images for radiation treatment planning, the patient has to be imaged in the same position for both CT and PET and ideally in the treatment position to prevent errors in target volume placement. Immobilization devices and the use of external room lasers during treatment delivery further increase accuracy. The growing experience with FDG PET for directing treatment planning provides the precedent for using other tracers for this purpose [63]. An example of this is presented later in this review. Traditionally, radiation treatment planning is based on GTV information from pretherapy imaging studies. However, as the tumor volume changes with continuing treatment, it is important that the process of target delineation and treatment modification should be a continuing process. Thus a “plan-of-the-day” concept sounds attractive in achieving an optimal image-guided radiotherapy, keeping the baseline study to start the treatment planning process, but we recognize that this places a large burden on both imaging and therapy planning and is probably some time in the future.

Hypoxia-based IMRT boost

The ability of radiotherapy techniques to deliver higher radiation doses to tissues at risk for failure is limited by normal tissue tolerance when conventional field and fractionation schemes are used. To circumvent this problem and deliver “boost” radiation to resistant tumors, several versions of boost radiation therapy based on this theme have been used [64–66]. Concomitant boost using a field within a field is one technique that has been used to boost the total tumor dose in 53 patients with advanced head and neck cancer. The authors achieved a 2-year regional control rate of 65% and a survival of 55% as compared with commonly reported results of 40% and 25%, respectively. Knowledge of regional hypoxia can also help target radiotherapy. Chao et al. successfully investigated the potential use of hypoxia-guided IMRT using a custom-designed anthropomorphic phantom and ^{64}Cu-ATSM PET imaging [20] but no human results have been reported. IMRT is ideal for providing boost radiation without the toxicity seen with earlier methods that precluded the routine clinical application of boost radiotherapy [67].

Case example: PET imaging to direct glioma radiotherapy

Hypoxia and gliomas

Studies of oxygen metabolism and blood flow in gliomas with PET and [^{15}O]O_2, [^{15}O]H_2O, and [^{15}O]CO have consistently shown that oxygen utilization is low relative to normal cortex despite an adequate supply of oxygen at least macroscopically, i.e., there are adequate blood flow and blood oxygen levels to meet the metabolic demands of the tumors[68–73]. The utilization of oxygen relative to that of glucose, namely the metabolic ratio, is reduced in malignant gliomas [71, 72]. In normal brain the metabolic ratio is 5.2 moles O_2 per mole glucose while in gliomas it is 1.9 [71, 74]. This low metabolic ratio indicates that the tumor breaks down glucose to lactate (glycolysis) and that non-oxidative metabolism of glucose is occurring. In the face of adequate blood flow and reduced oxygen extraction in tumors, the reduced metabolic ratio indicates that glycolysis is occurring under aerobic conditions [68].

The presence of hypoxia as a potential contributor to resistance to radio- and chemotherapy in malignant gliomas is now well established. Spontaneous necrosis observed in both gross and microscopic specimens provides graphic evidence for the presence of hypoxia [75, 76]. Rampling et al. proved that malignant astrocytic gliomas contain hypoxic regions by measurements with polarographic electrodes [77]. The percent Po_2 values <2.5 mmHg were 10–69% with a median of 40% in glioblastomas. In anaplastic

astrocytomas the percent Po_2 values <2.5 mmHg were 9–42% with a median of 20%.

Hypoxia imaging of gliomas

Reports of FMISO PET imaging of gliomas are emerging [78–81]. Liu reported that FMISO was taken up in 14/18 brain tumors [79] and Bruehlmeier et al. found increased uptake in 7/7 glioblastomas [78]. Scott's group studied 13 newly diagnosed patients prior to surgery with both FMISO and FDG PET [80]. There was a correlation between FMISO uptake and tumor grade, and all high-grade lesions showed uptake that was frequently heterogeneous. There was only partial overlap between regions of FMISO uptake and FDG uptake. An example shown in Fig. 1 demonstrates heterogeneous uptake that does not show conformity to the FDG region of uptake in these co-registered images.

These studies in aggregate show significant promise for FMISO PET in gliomas but need to be extended to a larger patient population examined at additional time points through the clinical course. Only then will the potential clinical value of this imaging method be determined. This may prove useful for identifying the regional distribution of hypoxia for planning tumor resections and targeting higher doses of RT more precisely to hypoxic areas.

PET-guided glioma radiotherapy

Conventional conformal radiotherapy (RT) for malignant gliomas consists of 1.8- to 2.0-Gy fractions administered to a total of around 60 Gy. Despite these doses, nearly inevitably there are in-field recurrences, progression and death. Doses as high as 70–90 Gy have been studied with the goals of overcoming resistance and providing better results than with 60 Gy [82–85]. There was no improvement in survival or local control, and recurrences developed in the volumes that received the high doses [83]. Treatment aimed at eradication of hypoxic tumor with RT plus hypoxic cell-radiosensitizing drugs has been unsuccessful [86–88]. Also, the use of fast neutron RT to overcome resistance due to hypoxia has proven to be too toxic to brain tissue [89]. From these studies it is obvious that a much better understanding is needed of the role of hypoxia in the poor response of gliomas to RT.

Some examples of using PET to direct glioma radiotherapy are emerging. Gross and co-workers incorporated FDG PET results with MRI for delineation of the three-dimensional 60-Gy treatment volumes for 18 high-grade gliomas [90]. The median survival of 310 days provided no improvement compared with other reports. They concluded that FDG PET did not add useful information for conventional treatment planning but suggested that FDG PET might prove useful to define a volume of tumor for a boost dose of RT. Such a study was in fact underway simultaneously in which FDG PET was being used to define the optimal volume for high-dose boost RT in glioblastoma [91]. Patients received 59.4 Gy in 33 fractions followed by an additional 20 Gy in 10 fractions directed at the FDG PET-defined volume of hypermetabolism plus a 0.5-cm margin. Although the median survival for the 40 patients in this trial was 70 weeks, this was not better than survival in historical controls. This pilot study showed that experimental RT protocols based on PET imaging are feasible and could in the future be designed to target regions of hypoxia. Other centers are beginning to explore the incorporation of FDG PET targeting for simultaneous integrated boost in IMRT [92] and for planning radiosurgery target volumes [93, 94]. Radiotherapy planning based on FDG PET or FMISO PET will of course need to produce improved treatment outcomes before it will be widely applied in clinical practice.

Case example: PET imaging to direct head and neck radiotherapy

In our ongoing research on imaging and characterizing hypoxia in head and neck cancer, we are investigating the role of FMISO PET imaging in guiding therapy. The patient in this example had biopsy-proven advanced carcinoma of the head and neck. The patient underwent baseline head and neck CT imaging. PET images were obtained at ~90 min following the injection of 0.1 mCi/kg of ^{18}F-FMISO. The patient also had whole-body FDG for staging and measurement of glucose metabolism as well as for staging. PET/CT image coregistration was achieved using the ADAC/

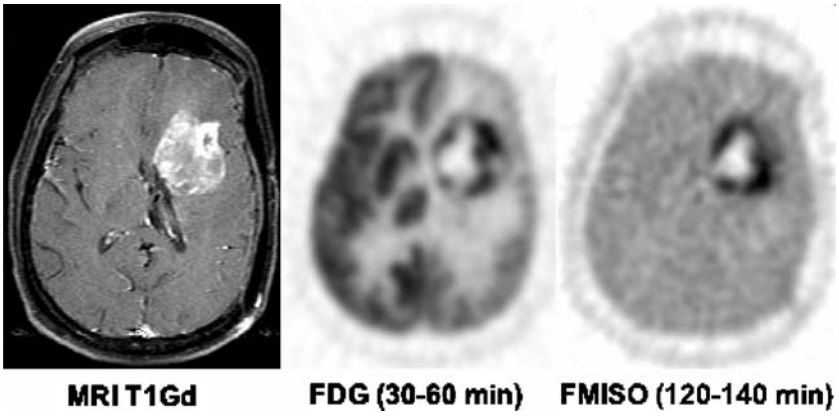

Fig. 1. Transaxial MR T1 Gd, FDG PET and FMISO PET images showing heterogeneous uptake that does not show conformity in the tumor

Pinnacle (Philips Medical Systems, Madison, WI, USA) Syntegra fusion package (rigid body). The coregistered images, as shown in Fig. 2, were used by the physician to guide the delineation of gross tumor volumes (GTVs). The FMISO PET images were used to determine hypoxic subvolumes for boost planning. GTVs were expanded or contracted, where appropriate, to form the planning target volume (PTV). The critical structures of interest included the parotid glands, spinal cord, and mandible. ADAC/Pinnacle radiation treatment planning software was used to build seven-beam IMRT treatment plans using 6-MV photon beams and inverse-planning techniques. Initial IMRT treatment prescribed 70 Gy to the PTV and 50 Gy to affected nodes, with constraints on homogeneity. Dose volume histogram (DVH) objectives follow the RTOG 00-22 trial specifications. The IMRT boost plan escalated the dose to the hypoxic subvolume by an additional 10 Gy. Target dose limits for critical structures used to guide the inverse planning included: spinal cord ≤45 Gy, mandible ≤70 Gy, and mean dose to parotid glands <26 Gy with ≤40 Gy to 40% of the volume of the ipsilateral gland and ≤20 Gy to 20% of the contralateral gland.

The isodose display of the composite plan in Fig. 3 shows the conformal isodoses around the targets and the sparing of critical structures and Fig. 4 presents the DVHs for the two plans i.e., with and without boost radiation for this patient. The hypoxic subvolume clearly receives the intended 10-Gy boost while remaining within the maximum dose objectives of the critical structures.

Summary

Pitfalls of hypoxia-guided radiotherapy

While hypoxia-directed treatment alone is not the answer to all causes of treatment failure, image-guided radiation dose escalation would help to overcome hypoxia-induced treatment resistance without the added toxicity of systemic agents. Additionally, since tumor hypoxia is a dynamic process that changes during the course of a treatment, it is important to establish the significance of pretherapy hypoxic subvolumes as well as changing hypoxic volumes during therapy as the target for boost radiation. Again, the need to provide margins around a target for delivery of effective treatment will limit how small the boost target volume should be. For smaller GTVs (e.g., 0.5-cm lymph node) it might not be possible to demarcate the subvolume with the GTV. Although the term BTV is used for a whole gamut of cellular functions, current radiation therapy practices are limited in addressing individual biological processes in an independent fashion. Even though dose escalation has been used clinically, radiobiological evidence for its role in controlling the hypoxic subvolume needs to be established in large clinical studies.

Conclusions and future directions

Tissue hypoxia is common in solid tumors and leads to cellular changes that confer aggressive behavior and therapeutic resistance. Although hypoxia induces resistance to a variety of treatments, the absence of oxygen is especially critical for photon radiotherapy, which depends upon the generation of free radicals for its cytotoxic effect. Identifying regions of tissue hypoxia and targeting them for higher doses of radiotherapy and possibly hypoxia-specific systemic therapy is key to improving the treatment of tumor types like glioblastoma , head/neck cancer, and cervical cancer, where hypoxia is common.

Methods for detecting tissue hypoxia have traditionally been invasive and required access to the tumor site, limiting their use in clinical practice. Furthermore, electrode or polarographic methods are subject to significant sampling

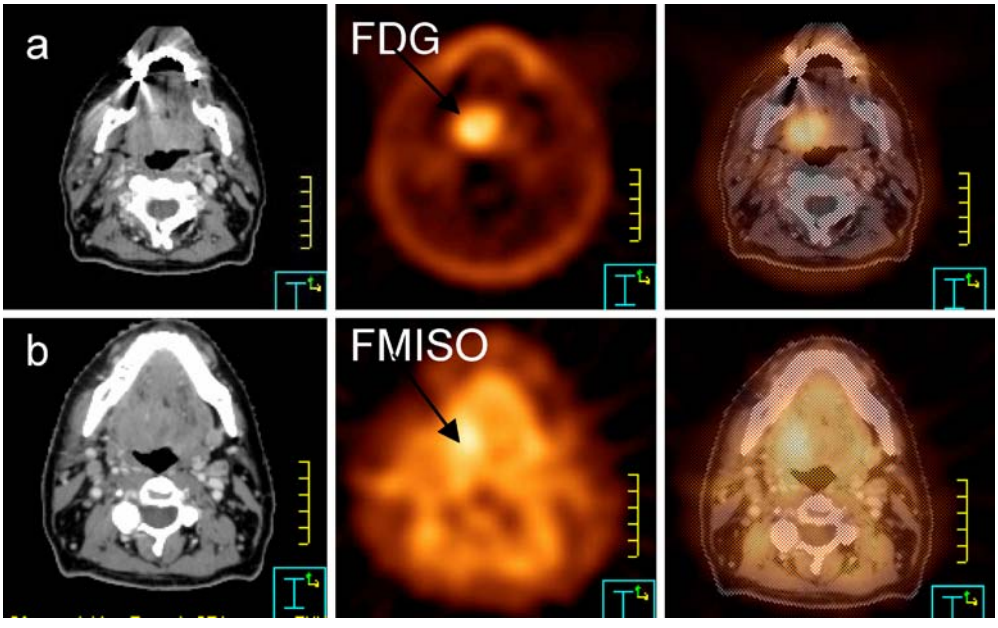

Fig. 2. Co-registration process. **a** Corresponding transaxial slice of CT, FDG PET, and fused CT/PET. Note the FDG uptake of the primary tumor (*FD, arrow*). **b** Corresponding slices of CT, FMISO PET, and fused CT/PET. Note the FMISO uptake of the hypoxic subvolume of the primary tumor (*FMIS, arrow*)

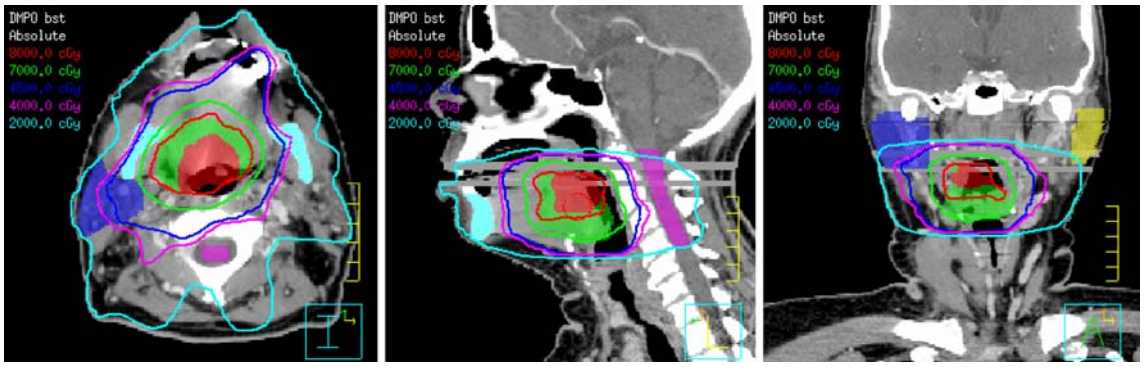

Fig. 3. Isodose map in transaxial, sagittal, and coronal projections of the composite IMRT plan. The primary PTV (*green*) was treated to 70 Gy, while the FMISO PTV (*red*) was treated with an additional 10-Gy boost in a consecutive plan. The ipsilateral parotid gland (*blue*) receives no more than 40 Gy to 40% of its volume. The contralateral parotid gland (*yellow*) receives no more than 20 Gy to 20% of its volume. The mandible (*sky blue*) is constrained to no more than 70 Gy. The cord (*pink*) is constrained to no more than 45 Gy

error in large and heterogeneous tumors. For these reasons, imaging has been used to detect and quantify tumor hypoxia with considerable initial success. A variety of hypoxia radiopharmaceuticals have been designed to have higher uptake in hypoxic versus non-hypoxic tumor. The nitroimidazole, FMISO, was one of the earliest compounds developed and has the largest existing body of experience for hypoxia imaging.

A number of studies in the literature have tested hypoxia imaging in preclinical animal models and in patients. A wide variety of tumors including brain, head/neck, cervix, lung, and breast have demonstrated significant hypoxia by PET imaging. Studies are emerging that confirm imaging measures of hypoxia as prognostic biomarkers, predictive of patient outcome, underscoring their potential to direct therapy. In general, neither clinical characteristics nor other imaging modalities can reliably identify tissue hypoxia. While hypoxia generally leads to increased glycolysis and increased FDG uptake, FDG uptake is not a measure of hypoxia.

Some examples are emerging that use functional PET imaging, combined with anatomic imaging, to direct radiotherapy. Most early efforts have used FDG PET to help plan radiotherapy, but some more recent preliminary studies are investigating the feasibility of radiotherapy treatment planning using hypoxia-specific PET imaging. The incorporation of biological imaging into radiotherapy treatment planning represents an important advance and future direction in cancer treatment. Clinical studies will need to evaluate the value of hypoxia imaging in directing radiotherapy. These studies will need to use both efficacy and toxicity as endpoints, as functional imaging may lead to improvements in either or both. This will call for new approaches to clinical study design, incorporating hypoxia imaging as a biomarker to direct tumor therapy.

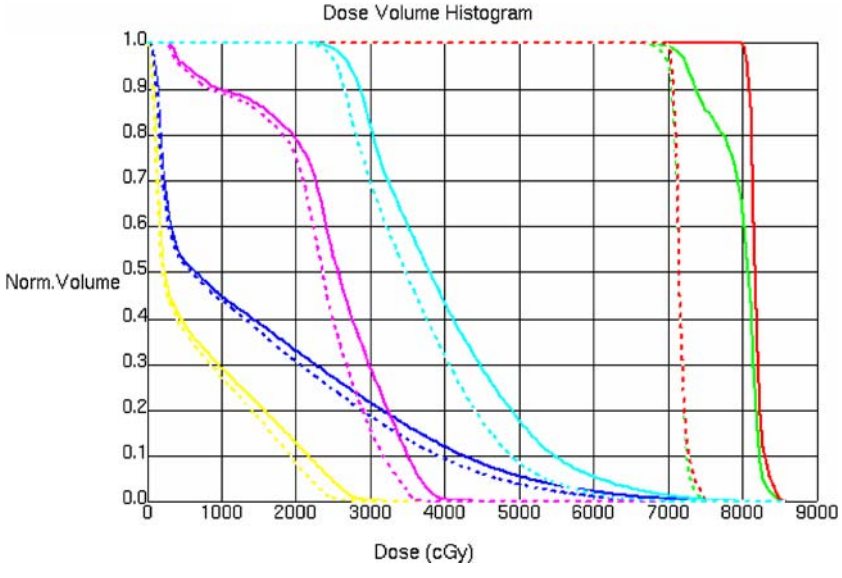

Fig. 4. Caption for DVH display: DVH of the initial treatment to 70 Gy (*dashed lines*) and composite plan (*solid lines*), including the boost of the FMISO target to an additional 10 Gy

Acknowledgements. The authors would like to thank the following for help provided towards conducting hypoxia imaging research: Lanell Peterson, Jeff Scharnhorst, Mark Philips, Janet Eary, all the nuclear medicine technologists, and Jean Link, Tom Adamson, and Steve Shoner.

This work was supported in part by NIH Grant P01CA42045 and S10 RR17229.

References

1. Thomlinson RH, Gray LH. The histological structure of some human lung cancers and the possible implications for radiotherapy. Br J Cancer 1955;9:537–549
2. Kourkourakis MI, Giatromanolaki A, Sivridis E, Fezoulidis I. Cancer vascularization: implications in radiotherapy? Int J Radiat Oncol Biol Phys 2000;48:545s–553s
3. Scandurro AB, Weldon CW, Figueroa YG, Alam J, Beckman BS. Gene microarray analysis reveals a novel hypoxia signal transduction pathway in human hepatocellular carcinoma cells. Int J Oncol 2001;19:129–135
4. Villaret DB, Wang T, Dillon D, Xu J, Sivam D, Cheever MA, et al. Identification of genes overexpressed in head and neck squamous cell carcinoma using a combination of complementary DNA subtraction and microarray analysis. Laryngoscope 2000;110:374–381
5. Rajendran JG, Wilson D, Conrad EU, Peterson LM, Bruckner JD, Rasey JS, et al. F-18 FMISO and F-18 FDG PET imaging in soft tissue sarcomas: correlation of hypoxia, metabolism and VEGF expression. Eur J Nuc Med Mol Imaging 2003;30: 695–704
6. Hockel M, Schlenger K, Hockel S, Vaupel P. Hypoxic cervical cancers with low apoptotic index are highly aggressive. Cancer Res 1999;59:4525–4528
7. Ivan M, Kondo K, Yang H, Kim W, Valiando J, Ohh M, et al. HIFalpha targeted for VHL-mediated destruction by proline hydroxylation: implications for O2 sensing. Science 2001; 292:464–468
8. Huang LE, Arany Z, Livingston DM, Bunn HF. Activation of hypoxia-inducible transcription factor depends primarily upon redox-sensitive stabilization of its alpha subunit. J Biol Chem 1996;271:32253–32259
9. Guillemin K, Krasnow MA. The hypoxic response: huffing and HIFing. Cell 1997;89:9–12
10. Clavo AC, Wahl RL. Effects of hypoxia on the uptake of tritiated thymidine, L-leucine, L-methionine and FDG in cultured cancer cells. J Nucl Med 1996;37:502–506
11. Burgman P, Odonoghue JA, Humm JL, Ling CC. Hypoxia-induced increase in FDG uptake in MCF7 cells. J Nucl Med 2001;42:170–175
12. Rajendran JG, Mankoff DA, O'Sullivan F, Peterson LM, Schwartz DL, Conrad EU, et al. Hypoxia and glucose metabolism in malignant tumors: evaluation by [^{18}F]fluoromisonidazole and [^{18}F]fluorodeoxyglucose positron emission tomography imaging. Clin Cancer Res 2004;10:2245–2252
13. Hall EJ. Radiobiology for the radiologist. Lippincott Williams & Wilkins, Philadelphia, PA; 2000
14. Marples B, Greco O, Joiner MC, Scott SD. Molecular approaches to chemo-radiotherapy. Eur J Cancer 2002;38:231–239
15. Overgaard J, Horsman MR. Modification of hypoxia-induced radioresistance in tumors by the use of oxygen and sensitizers. Semin Radiat Oncol 1996;6:10–21
16. Fowler JF. Eighth annual Juan del Regato lecture. Chemical modifiers of radiosensitivity—theory and reality: a review. Int J Radiat Oncol Biol Phys 1985;11:665–674
17. Evans SM, Koch CJ. Prognostic significance of tumor oxygenation in humans. Cancer Lett 2003;195:1–16
18. Moulder JE, Rockwell S. Tumor hypoxia: its impact on cancer therapy. Cancer Metastasis Rev 1987;5:313–341
19. Rajendran JG, Meyer J, Schwartz DL, Kinahan PE, Cheng P, Hummel SM, et al. Imaging with F-18 FMISO-PET permits hypoxia directed radiotherapy dose escalation for head and neck cancer. J Nucl Med 2003;44:415, 127P
20. Chao KS, Bosch WR, Mutic S, Lewis JS, Dehdashti F, Mintun MA, et al. A novel approach to overcome hypoxic tumor resistance: Cu-ATSM-guided intensity-modulated radiation therapy. Int J Radiat Oncol Biol Phys 2001;49:1171–1182
21. Brown JM. Exploiting the hypoxic cancer cell: mechanisms and therapeutic strategies. Mol Med Today 2000;6:157–162
22. Lee DJ, Moini M, Giuliano J, Westra WH. Hypoxic sensitizer and cytotoxin for head and neck cancer. Ann Acad Med Singapore 1996;25:397–404
23. Rischin D, Peters L, Hicks R, Hughes P, Fisher R, Hart R, et al. Phase I trial of concurrent tirapazamine, cisplatin, and radiotherapy in patients with advanced head and neck cancer. J Clin Oncol 2001;19:535–542
24. Rasey JS, Casciari JJ, Hofstrand PD, Muzi M, Graham MM, Chin LK. Determining hypoxic fraction in a rat glioma by uptake of radiolabeled fluoromisonidazole. Radiat Res 2000; 153:84–192
25. Prekeges JL, Rasey JS, Grunbaum Z, Krohn KH. Reduction of fluoromisonidazole, a new imaging agent for hypoxia. Biochem Pharmacol 1991;42:2387–2395
26. Chapman JD, Engelhardt EL, Stobbe CC, Schneider RF, Hanks GE. Measuring hypoxia and predicting tumor radioresistance with nuclear medicine assays. Radiother Oncol 1998; 46:229–237
27. Grierson JR, Link JM, Mathis CA, Rasey JS, Krohn KA. Radiosynthesis of fluorine-18 fluoromisonidazole. J Nucl Med 1989;30:343–350
28. Rasey JS, Koh WJ, Evans ML, Peterson LM, Lewellen TK, Graham MM, et al. Quantifying regional hypoxia in human tumors with positron emission tomography of [^{18}F]fluoromisonidazole: a pretherapy study of 37 patients. Int J Radiat Oncol Biol Phys 1996;36:417–428
29. Rajendran JG, Mankoff DA, O'Sullivan F, Peterson LM, Schwartz DL, Conrad EU, Spence AM, Muzi M, Farwell DG, Krohn, KA. Hypoxia and glucose metabolism in malignant tumors: evaluation by [^{18}F]fluoromisonidazole and [^{18}F] fluorodeoxyglucose positron emission tomography imaging. Clin Cancer Res 2004;10:2245–2252
30. Liu RS, Chu LS, Yen SH, Chang CP, Chou KL, Wu LC, et al. Detection of anaerobic odontogenic infections by fluorine-18 fluoromisonidazole. Eur J Nucl Med 1996;23:1384–1387
31. Bentzen L, Keiding S, Horsman MR, Falborg L, Hansen SB, Overgaard J. Feasibility of detecting hypoxia in experimental mouse tumours with ^{18}F-fluorinated tracers and positron emission tomography—a study evaluating [^{18}F]fluoro-2-deoxy-D-glucose. Acta Oncol 2000;39:629–637
32. Yeh SH, Liu RS, Wu LC, Yang DJ, Yen SH, Chang CW, et al. Fluorine-18 fluoromisonidazole tumour to muscle retention ratio for the detection of hypoxia in nasopharyngeal carcinoma. Eur J Nucl Med 1996;23:1378–1383
33. Koch CJ, Evans SM. Non-invasive PET and SPECT imaging of tissue hypoxia using isotopically labeled 2-nitroimidazoles. Adv Exp Med Biol 2003;510:285–292
34. Piert M, Machulla HJ, Picchio M, Reischl G, Ziegler S, Kumar P, et al. Hypoxia-specific tumor imaging with ^{18}F-fluoroazomycin arabinoside. J Nucl Med 2005;46:106–113

35. Fujibayashi Y, Taniuchi H, Yonekura Y, Ohtani H, Konishi J, Yokoyama A. Copper-62-ATSM: a new hypoxia imaging agent with high membrane permeability and low redox potential. J Nucl Med 1997;38:1155–1160
36. Lewis JS, McCarthy DW, McCarthy TJ, Fujibayashi Y, Welch MJ. Evaluation of Cu-64-ATSM in vitro and in vivo in a hypoxic model. J Nucl Med 1999;40:177–183
37. Ballinger JR. Imaging hypoxia in tumors. Semin Nucl Med 2001;31:321–329
38. O'Donoghue JA, Zanzonico P, Pugachev A, Wen B, Smith-Jones P, Cai S, et al. Assessment of regional tumor hypoxia using ^{18}F-fluoromisonidazole and ^{64}Cu(II)-diacetyl-bis(N^4-methylthiosemicarbazone) positron emission tomography: comparative study featuring microPET imaging, Po2 probe measurement, autoradiography, and fluorescent microscopy in the R3327-AT and FaDu rat tumor models. Int J Radiat Oncol Biol Phys 2005;61:1493–1502
39. Hanks GE, Hanlon AL, Schultheiss TE, Pinover WH, Movsas B, Epstein BE, et al. Dose escalation with 3D conformal treatment: five year outcomes, treatment optimization, and future directions. Int J Radiat Oncol Biol Phys 1998;41:501–510
40. Zelefsky MJ, Leibel SA, Kutcher GJ, Fuks Z. Three-dimensional conformal radiotherapy and dose escalation: where do we stand? Semin Radiat Oncol 1998;8:107–114
41. Dogan N, Leybovich LB, Sethi A, Emami B. Improvement of dose distributions in abutment regions of intensity modulated radiation therapy and electron fields. Med Phys 2002;29:38–44
42. Svensson H, Moller TR. Developments in radiotherapy. Acta Oncol 2003;42:430–442
43. Williams PC. IMRT: delivery techniques and quality assurance. Br J Radiol 2003;76:766–776
44. Webb S. The physical basis of IMRT and inverse planning. Br J Radiol 2003;76:678–689
45. Verhey LJ. Issues in optimization for planning of intensity-modulated radiation therapy. Semin Radiat Oncol 2002;12: 210–218
46. Goffman TE, Glatstein E. Intensity-modulated radiation therapy. Radiat Res 2002;158:115–117
47. Intensity Modulated Radiation Therapy Collaborative Working Group. Intensity-modulated radiotherapy: current status and issues of interest. Int J Radiat Oncol Biol Phys 2001;51: 880–914
48. Garden AS, Morrison WH, Rosenthal DI, Chao KS, Ang KK. Target coverage for head and neck cancers treated with IMRT: review of clinical experiences. Semin Radiat Oncol 2004;14: 103–109
49. Eisbruch A, Foote RL, O'Sullivan B, Beitler JJ, Vikram B. Intensity-modulated radiation therapy for head and neck cancer: emphasis on the selection and delineation of the targets. Semin Radiat Oncol 2002;12:238–249
50. Alber M, Paulsen F, Eschmann SM, Machulla HJ. On biologically conformal boost dose optimization. Phys Med Biol 2003; 48:N31–N35
51. Chao KS, Low DA, Perez CA, Purdy JA. Intensity-modulated radiation therapy in head and neck cancers: the Mallinckrodt experience. Int J Cancer 2000;90:92–103
52. Ling CC, Humm J, Larson S, Amols H, Fuks Z, Leibel S, et al. Towards multidimensional radiotherapy (MD-CRT): biological imaging and biological conformality. Int J Radiat Oncol Biol Phys 2000;47:551–560
53. Mankoff DA, Shields AF, Krohn KA. PET imaging of cellular proliferation. Radiol Clin North Am 2005;43:153–167
54. Rajendran JG, Schwartz DS, O'Sullivan J, Peterson LM, Ng P, Scarnhorst J, et al. Tumor hypoxia imaging with [F-18]FMISO PET in head and neck cancer: value of pre-therapy FMISO uptake in predicting survival. Clin Cancer Res; 2006; in press
55. Rajendran JG, Krohn KA. Imaging hypoxia and angiogenesis in tumors. Radiol Clin North Am 2005;43:169–187
56. Eschmann SM, Paulsen F, Reimold M, Dittmann H, Welz S, Reischl G, et al. Prognostic impact of hypoxia imaging with ^{18}F-misonidazole PET in non-small cell lung cancer and head and neck cancer before radiotherapy. J Nucl Med 2005;46: 253–260
57. Schwartz DL, Ford EC, Rajendran J, Yueh B, Coltrera MD, Virgin J, et al. FDG-PET/CT-guided intensity modulated head and neck radiotherapy: a pilot investigation. Head Neck 2005; 27:478–487
58. Yap JT, Carney JP, Hall NC, Townsend DW. Image-guided cancer therapy using PET/CT. Cancer J 2004;10:221–233
59. Heron DE, Andrade RS, Flickinger J, Johnson J, Agarwala SS, Wu A, et al. Hybrid PET-CT simulation for radiation treatment planning in head-and-neck cancers: a brief technical report. Int J Radiat Oncol Biol Phys 2004;60:1419–1424
60. Esthappan J, Mutic S, Malyapa RS, Grigsby PW, Zoberi I, Dehdashti F, et al. Treatment planning guidelines regarding the use of CT/PET-guided IMRT for cervical carcinoma with positive paraaortic lymph nodes. Int J Radiat Oncol Biol Phys 2004;58:1289–1297
61. Thorwarth D, Eschmann SM, Paulsen F, Alber M. A kinetic model for dynamic [^{18}F]-Fmiso PET data to analyse tumour hypoxia. Phys Med Biol 2005;50:2209–2224
62. Thorwarth D, Eschmann SM, Scheiderbauer J, Paulsen F, Alber M. Kinetic analysis of dynamic ^{18}F-fluoromisonidazole PET correlates with radiation treatment outcome in head-and-neck cancer. BMC Cancer 2005;5:152
63. Grosu AL, Piert M, Weber WA, Jeremic B, Picchio M, Schratzenstaller U, et al. Positron emission tomography for radiation treatment planning. Strahlenther Onkol 2005;181: 483–499
64. Mehta VK, Poen JC, Ford JM, Oberhelman HA, Vierra MA, Bastidas AJ, et al. Protracted venous infusion 5-fluorouracil with concomitant radiotherapy compared with bolus 5-fluorouracil for unresectable pancreatic cancer. Am J Clin Oncol 2001;24:155–159
65. Johnson CR, Schmidt-Ullrich RK, Wazer DE. Concomitant boost technique using accelerated superfractionated radiation therapy for advanced squamous cell carcinoma of the head and neck. Cancer 1992;69:2749–2754
66. Grills IS, Yan D, Martinez AA, Vicini FA, Wong JW, Kestin LL. Potential for reduced toxicity and dose escalation in the treatment of inoperable non-small-cell lung cancer: a comparison of intensity-modulated radiation therapy (IMRT), 3D conformal radiation, and elective nodal irradiation. Int J Radiat Oncol Biol Phys 2003;57:875–890
67. Ahmed RS, Kim RY, Duan J, Meleth S, De Los Santos JF, Fiveash JB. IMRT dose escalation for positive para-aortic lymph nodes in patients with locally advanced cervical cancer while reducing dose to bone marrow and other organs at risk. Int J Radiat Oncol Biol Phys 2004;60:505–512
68. Allen N. Respiration and oxidative metabolism of brain tumors. In: Kirsch WM, Paoletti EG, Paoletti P, editors. The experimental biology of brain tumors. Springfield: Charles C. Thomas;, 1972. p 243–274
69. Ito M, Lammertsma AA, Wise RJ, Bernardi S, Frackowiak RS, Heather JD, et al. Measurement of regional cerebral blood flow and oxygen utilisation in patients with cerebral tumours using ^{15}O and positron emission tomography: analytical techniques and preliminary results. Neuroradiology 1982;23:63–74
70. Lammertsma AA, Frackowiak RS. Positron emission tomography. Crit Rev Biomed Eng 1985;13:125–169
71. Rhodes CG, Wise RJ, Gibbs JM, Frackowiak RS, Hatazawa J, Palmer AJ, et al. In vivo disturbance of the oxidative metabolism of glucose in human cerebral gliomas. Ann Neurol 1983;14:614–626

72. Tyler JL, Diksic M, Villemure JG, Evans AC, Meyer E, Yamamoto YL, et al. Metabolic and hemodynamic evaluation of gliomas using positron emission tomography. J Nucl Med 1987;28:1123–1133
73. Wise RJS, Thomas DGT, Lammertsma AA, Rhodes CG. PET scanning of human brain tumors. Prog Exp Tumor Res 1984; 27:154–169
74. Baron JC, Rougemont D, Soussaline F, Bustany P, Crouzel C, Bousser MG, et al. Local interrelationships of cerebral oxygen consumption and glucose utilization in normal subjects and in ischemic stroke patients: a positron tomography study. J Cereb Blood Flow Metab 1984;4:140–149
75. Brat DJ, Castellano-Sanchez AA, Hunter SB, Pecot M, Cohen C, Hammond EH, et al. Pseudopalisades in glioblastoma are hypoxic, express extracellular matrix proteases, and are formed by an actively migrating cell population. Cancer Res 2004;64: 920–927
76. Evans SM, Judy KD, Dunphy I, Jenkins WT, Nelson PT, Collins R, et al. Comparative measurements of hypoxia in human brain tumors using needle electrodes and EF5 binding. Cancer Res 2004;64:1886–1892
77. Rampling R, Cruickshank G, Lewis AD, Fitzsimmons SA, Workman P. Direct measurement of pO2 distribution and bioreductive enzymes in human malignant brain tumors. Int J Radiat Biol Phys 1994;29:427–431
78. Bruehlmeier M, Roelcke U, Schubiger PA, Ametamey SM. Assessment of hypoxia and perfusion in human brain tumors using PET with ^{18}F-fluoromisonidazole and ^{15}O-H_2O. J Nucl Med 2004;45:1851–1859
79. Liu Q. Constriction to hypoxia-reoxygenation in isolated mouse coronary arteries: role of endothelium and superoxide. J Appl Physiol 1999;87:1392–1396
80. Scott AM, Ramdave S, Hannah A, Pathmaraj K, Tochon-Danguy H, Sachinidis J, et al. Correlation of hypoxic cell fraction with glucose metabolic rate in gliomas with ^{18}F-fluoromisonidazole (FMISO) and ^{18}F-fluorodeoxyglucose (FDG) positron emission tomography (PET). J Nucl Med 2001;42:abstract 250, 267P
81. Valk P, Mathis C, Prados M, Gilbert J, Budinger T. Hypoxia in human gliomas: demonstration by PET with fluorine-18-fluoromisonidazole. J Nucl Med 1992;33:2133–2137
82. Chang CH, Horton J, Schoenfeld D, Salazer O, Perez-Tamayo R, Kramer S, et al. Comparison of postoperative radiotherapy and combined postoperative radiotherapy and chemotherapy in the multidisciplinary management of malignant gliomas. A joint Radiation Therapy Oncology Group and Eastern Cooperative Oncology Group study. Cancer 1983;52:997–1007
83. Lee SW, Fraass BA, Marsh LH, Herbort K, Gebarski SS, Martel MK, et al. Patterns of failure following high-dose 3-D conformal radiotherapy for high-grade astrocytomas: a quantitative dosimetric study. Int J Radiat Oncol Biol Phys 1999;43:79–88
84. Nelson DF, Diener-West M, Horton J, Chang CH, Schoenfeld D, Nelson JS. Combined modality approach to treatment of malignant gliomas—re-evaluation of RTOG 7401/ECOG 1374 with long-term follow-up: a joint study of the Radiation Therapy Oncology Group and the Eastern Cooperative Oncology Group. NCI Monogr 1988;6:279–284
85. Salazar OM, Rubin P, Feldstein ML, Pizzutiello R. High dose radiation therapy in the treatment of malignant gliomas: final report. Int J Radiat Oncol Biol Phys 1979;5:1733–1740
86. Davis LW. Malignant glioma—a nemesis which requires clinical and basic investigation in radiation oncology. Int J Radiat Oncol Biol Phys 1989;16:1355–1365
87. Green SB, Byar DP, Strike TA, Alexander E, Brooks WH, Burger PC, et al. Randomized comparisons of BCNU, streptozotocin, radiosensitizer, and fractionation of radiotherapy in the post-operative treatment of malignant glioma. Proc ASCO 1984;3:260
88. Nelson DF, Schoenfeld D, Weinstein AS, Nelson JS, Wasserman T, Goodman RL, et al. A randomized comparison of misonidazole sensitized radiotherapy plus BCNU and radiotherapy plus BCNU for treatment of malignant glioma after surgery; preliminary results of an RTOG study. Int J Radiat Oncol Biol Phys 1983;9:1143–1151
89. Griffin TW, Davis R, Laramore G, Hendrickson F, Rodrigues Antunez A, Hussey D, et al. Fast neutron radiation therapy for glioblastoma multiforme. Results of an RTOG study. Am J Clin Oncol 1983;6:661–667
90. Gross MW, Weber WA, Feldmann HJ, Bartenstein P, Schwaiger M, Molls M. The value of F-18-fluorodeoxyglucose PET for the 3-D radiation treatment planning of malignant gliomas. Int J Radiat Oncol Biol Phys 1998;41:989–995
91. Douglas JG, Stelzer KJ, Mankoff DA, Tralins KS, Krohn KA, Muzi M, et al. [F-18]-fluorodeoxyglucose positron emission tomography for targeting radiation dose escalation for patients with glioblastoma multiforme: clinical outcomes and patterns of failure. Int J Radiat Oncol Biol Phys 2006;64:886–891
92. Suzuki M, Nakamatsu K, Kanamori S, Okumra M, Uchiyama T, Akai F, Nishimura Y. Feasibility study of the simultaneous integrated boost (SIB) method for malignant gliomas using intensity-modulated radiotherapy (IMRT). Jpn J Clin Oncol 2003;33:271–277
93. Levivier M, Massager N, Wikler D, Lorenzoni J, Ruiz S, Devriendt D, et al. Use of stereotactic PET images in dosimetry planning of radiosurgery for brain tumors: clinical experience and proposed classification. J Nucl Med 2004;45:1146–1154
94. Solberg TD, Agazaryan N, Goss BW, Dahlbom M, Lee SP. A feasibility study of ^{18}F-fluorodeoxyglucose positron emission tomography targeting and simultaneous integrated boost for intensity-modulated radiosurgery and radiotherapy. J Neurosurg 2004;101(Suppl 3):381–389